# Electrophoretic Mobility of Wormlike Chains. 2. Theory

**Robert L. Cleland**†

*Department of Chemistry, Dartmouth College, Hanover, New Hampshire 03755*

*Received November 7, 1990; Revised Manuscript Received February 26, 1991*

ABSTRACT: The theoretical reduced electrophoretic mobility $u'$ of a wormlike cylinder having discrete sites along its axis is proportional, in the long-chain limit, to the average electrostatic potential $\langle\psi\rangle$ on the surface of shear. The proportionality constant is the same as that for the uniformly charged cylinder (UCC). Short chains are predicted to have somewhat smaller $u'$ values due to end effects. The treatment, which neglects ion-atmosphere relaxation, uses the Burgers method and the Yamakawa–Fujii chain model. As for the latter, the adjustable parameters are the Kuhn length, $A_K$, and the cylinder radius, $a$, which can be determined independently from hydrodynamic data evaluated in terms of the same model. The computed value of $u'$ then depends only on linear charge density along the chain contour and the method chosen to evaluate the surface potential. Numerical integration with use of the Debye–Hückel assumptions for the hyaluronate polyion ($a$ = 0.55 nm) leads to predicted $u'$ values for unperturbed ($A_K$ = 8.7 nm), expanded (or "frozen-worm"), and rodlike models of the polyion. Corrections for the nonlinear effects of the Poisson–Boltzmann potential and ion-atmosphere relaxation, as computed for the UCC, lead to good agreement for the expanded model with experimental results for hyaluronate. Use of the same chain parameters leads to similarly good agreement with experiment for polysaccharides (polygalacturonate, alginate, and chondroitin 4-sulfate) having one charge per monosaccharide unit. The UCC model having the same value of $a$ gives slightly lower results for $u'$. The discrete-site wormlike model predicts more accurately than the UCC model the ratio of $u'$ to the slope $m \equiv (\Delta pK/\Delta\alpha)_I$ of plots of the apparent dissociation constant p$K$ against degree of dissociation $\alpha$ from potentiometric titration. The discrepancy results from inclusion of self-energy of charge formation in the charging free energy traditionally used to interpret $m$ in terms of the UCC model.

## Introduction

The uniformly charged cylinder model of polyelectrolytes provides a definite prediction concerning the relation between the electrophoretic mobility and potentiometric titration. An experimental investigation[1] of the mobility of sodium hyaluronate in free solution gave values about 50% larger than those predicted by this model for the cylinder radius providing the best fit for potentiometric titration of hyaluronic acid.[2] This discrepancy can be greatly reduced by use of a better model. A treatment of electrophoresis based on the hydrodynamic model[3] of the wormlike chain is presented here which is consistent both with a previous treatment of potentiometric titration[4] and with experimental observations by these two methods. As background for this treatment a brief review of the closely related theory of electrophoretic mobility of charged particles of simple shape is appropriate.

**Electrophoresis of Spherical Particles.** In the course of the classical investigations of Debye and Hückel[5] into the conductivity of electrolyte solutions, Hückel[6] derived the electrophoretic velocity **U** (relative to the solvent velocity) for spherical particles by the methods of hydrodynamics for slow, steady fluid motion. When the external field $\mathbf{E}_0$ in the solution is assumed (Hückel approximation) to be everywhere parallel to the $x$ direction (unit vector **i**), $\mathbf{E}_0 = X\mathbf{i}$, where $X$ is the electric field intensity and **U** and the corresponding mobility $u$ are given by

$$\mathbf{U} = u\mathbf{E}_0 = D\psi_a X\mathbf{i}/6\pi\eta \qquad (1)$$

In eq 1 $\eta$ is the bulk viscosity and $D$ the bulk dielectric constant of the solvent, while $\psi_a$ is the (uniform) electrostatic (or $\zeta$) potential at the surface of shear of the particle. The coordinate system has its usual origin at the center of the sphere, whose surface is placed at the value $r = a$ of the radial vector **r**. Since the hydrodynamic equations treat the solvent as a structureless continuum with a sticking boundary condition at the particle surface, the radius $a$ clearly includes any adhering solvent layer.

Although Debye and Hückel claimed that eq 1 held for charged spherical particles generally, Henry[7] later showed that their result was restricted to the case that the particle had the same electrical conductivity as the solvent. For the nonconducting charged sphere, the validity of eq 1 was shown to be limited to the case $\kappa a \ll 1$, i.e., the particle radius $a$ much smaller than the Debye radius $\kappa^{-1}$, where $\kappa$ has its usual definition for 1:1 electrolytes:

$$\kappa \equiv (4\pi e^2 n/DVk_BT)^{1/2} \qquad (2)$$

In eq 2 $e$ is the elementary proton charge, $k_B$ is Boltzmann's constant, $T$ is the absolute temperature, and $n$ is the number of charged particles in volume $V$. The original assumption of Hückel concerning $\mathbf{E}_0$ does not hold when $a$ is not small compared to $\kappa^{-1}$, due to distortion of the applied field by the particle.

The investigations of Hückel[6] and Henry[7] dealt only with the "electrophoretic" effect of the relative motion of the central charged particle and its ionic atmosphere. Another perturbing effect of the atmosphere results from the distortion of its average radial symmetry about the particle, the so-called "relaxation" effect. Both effects normally reduce the magnitude of **U** from its limiting value (at $\kappa = 0$) in the absence of the atmosphere. The classic treatment of the relaxation effect for electrolyte solutions began with the work of Debye and Hückel[5] and was much improved by the revised version of Onsager.[8]

Developments in this field have been reviewed by many authors. A particularly useful review for the present work has been that of Overbeek and Wiersema.[9] The latter review discussed the authors' work with Loeb on the numerical solution of the hydrodynamic (Navier–Stokes) equation for spherical particles to include relaxation effects by allowing for perturbation of the ion atmosphere in an external field.[10]

† Present address: Department of Physical and Inorganic Pharmaceutical Chemistry, Biomedicum, Box 574, S-75123 Uppsala, Sweden.

0024-9297/91/2224-4391$02.50/0 

**Electrophoresis of Cylinders.** Although it has important applications to the problems of classical colloid chemistry, the impenetrable sphere model is of limited interest for the study of chain polyelectrolytes. Circular cylinder models, on the other hand, have been applied to advantage in the theoretical interpretation of both thermodynamic and kinetic properties of polyions, particularly following the considerable success of the classic uniform line-charge model of Manning.[11]

The electrophoretic mobility of infinitely long uniformly charged cylinders was also investigated by Henry[7] for the same conditions as for spheres. For cylinders migrating in a field $\mathbf{E}_0$ parallel to the cylinder axis, he obtained von Smoluchowski's classic result:[12] $\mathbf{U} = u_{\parallel}X\mathbf{i}$, in which $4\pi$ replaces $6\pi$ in eq 1. With the cylinder axis transverse to the applied field, Henry obtained an integral for $\mathbf{U} = u_{\perp}X\mathbf{i}$, whose numerical evaluation by Gorin[13] assumed the form

$$u_{\perp} = D\psi_a h(\kappa a)/8\pi\eta \tag{3}$$

where the function $h(\kappa a)$, although equal to unity for the case of equal conductivity, increased for the nonconducting cylinder from unity ($\kappa a = 0$) to 2 ($\kappa a = \infty$). For random orientation of the cylinder, Gorin averaged the *resistances* (i.e., the reciprocal mobilities) to obtain

$$(u_{cyl})^{-1} = \frac{1}{3}(u_{\parallel})^{-1} + \frac{2}{3}(u_{\perp})^{-1} \tag{4}$$

Schellman and Stigter,[14] quoting a supporting argument of de Keizer et al.,[15] preferred to average the mobilities directly to obtain $u_{cyl}$ for the random case

$$u_{cyl} = \frac{1}{3}u_{\parallel} + \frac{2}{3}u_{\perp} = \frac{D\psi_a f}{6\pi\eta} \tag{5}$$

where $f = [1 + h(\kappa a)]/2$. With this averaging eq 5 is identical with eq 1 for $\kappa a \ll 1$ and can be used with the factor $f$ to express deviations for both particle shapes. Over the range of $\kappa a$ from 0 to 0.4 of practical interest in this work, $f$ due to field distortion decreased from unity, as given by the Hückel approximation, by less than 3% for cylinders[13] and 1% for spheres[7] when the Debye–Hückel (DH) approximation[5] to the potential was used. Stigter[16] performed a revised numerical evaluation of $h(\kappa a)$ by adapting to cylinders the mathematical treatment of Wiersema et al.[10] for spherical particles mentioned above. Equation 5 may be rewritten

$$u' = y_0 f$$
$$y_0 \equiv |\psi_a|e/kT \tag{6}$$

in terms of the dimensionless parameters $y_0$, defined by the second equality of eq 6, and a reduced mobility $u'$, defined by

$$u' \equiv 6\pi\eta e|u|/DkT \tag{7}$$

At 25 °C, $u' = 0.750 \times 10^4|u|$ (for $u$ in cm$^2$ V$^{-1}$ s$^{-1}$), when values of $\eta$ and $D$ for water are used.

**Polyion Models.** Other early physical models that dealt with the electrophoretic mobility of polyelectrolytes[17-19] represented the situation in terms of a porous sphere (radius $S$) of uniform (volume) charge density. These theories predicted a free-draining result for the mobility at large $\kappa S$. For sufficiently large molecular weight $M_r$ the *experimental* mobility is independent of $M_r$ at any given ionic strength for essentially all chain polyions. This fact can be interpreted as confirming the free-draining character of the motion. Since the ionic strength dependence of the mobility predicted by the early theories depends only on $\kappa S$, however, the porous-sphere models failed to account for the dependence on ionic strength observed experimentally. This is especially true for a polyion of low charge density, such as hyaluronate, whose relatively small *linear* charge density, combined with a stiff molecular coil, maintains $\kappa S$ at the free-draining limit at all values of $\kappa$ for which measurements can be made. When the estimates for this comparison were made, the radius $S$ was taken to be the Flory hydrodynamic radius or the average root-mean-square radius from light scattering.

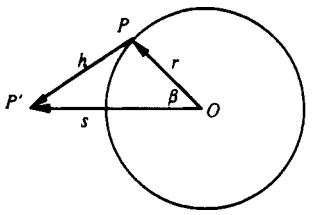


**Figure 1.** Vector diagram used to represent perturbations of the fluid velocity due to electrostatic forces in the Oseen formulation.

As Manning[20] has pointed out, the failure of the porous-sphere models is due to the fact that the actual distribution of the counterions in a polyion does not produce a *uniform* charge density throughout the polymer coil. Consideration of the observed experimental dependence of $u$ on $\kappa$ recalls rather the electrophoretic behavior of small ions, a fact which clearly suggests that the counterion distribution about the individual polyion charges should be considered in detail. Theoretical models which do just this, such as the continuous charge line or cylinder models of uniform charge density or discrete-charge models based on the actual polymeric chain have proved to be much more successful than the porous-sphere models in describing polyelectrolyte properties of coiling polyions.

The discrete-site model of polyion electrophoresis due to Manning,[20] which is a bead model based on the hydrodynamic treatments of Kirkwood and Riseman[21] and Kirkwood,[22] leads also to the result of eq 1 when we ignore the relaxation effect and limit attention to the high linear charge densities characteristic of counterion condensation. The results of this model, which provided the inspiration for the present work, will be compared later with our results.

**Theoretical Treatment.** Since the experiments of interest focus on polyions of polysaccharide character, we wish to use a chain model appropriate to such species. An examination[23] of the physical properties of hyaluronate has led to a preference for the wormlike chain model[24] for this purpose. A convenient choice for the investigation of hydrodynamic interactions is the wormlike cylinder employed by Yamakawa and Fujii,[3] within which the fixed polyion charges may be represented by discrete sites. In the following treatment estimates will be made of velocity perturbations in the fluid surrounding the polyion due to (1) the action of the external electrostatic field on the mobile charge distribution and (2) hydrodynamic interactions of the wormlike cylinder elements. To simplify the mathematical treatment, the charge distribution in the fluid will be assumed spherically symmetric about each fixed charged site of the polyion, while the fixed sites themselves will be taken to be equally spaced along the cylinder axis. The physical significance of these approximations will be considered under Discussion.

**Electrostatic Field Perturbations.** We consider the hydrodynamic effect of application of an external electric field $\mathbf{E}_0 = X\mathbf{i}$ to a charge distribution about a charged site located at the origin of coordinates $O$. The velocity perturbation $\mathbf{v}'$ is desired at a point $P'$ (see Figure 1) due to the point forces per unit volume $\mathbf{G} = \rho\mathbf{E}$ acting on volume elements having charge density $\rho$. When the total electric

field **E** is assumed to be a superposition of $\mathbf{E}_0$ and the local static field **E'** due to the polyion and the mobile charges, the effect of **E'** can be neglected when distortion of the equilibrium charge distribution by the applied field (relaxation effect) is ignored. In that case **v'** is given, according to the Oseen formulation,[25] as a sum over volume elements at all points $P$ by

$$\mathbf{v}' = \int_V \mathbf{TG}\, dV = \int \frac{\rho X\, dV}{8\pi\eta h}\left(\mathbf{I} + \frac{\mathbf{hh}}{h^2}\right)\mathbf{i}$$
$$= \int_{r=0}^{r=\infty}\int_{\beta=0}^{\beta=\pi}\frac{\rho X}{4\eta h}\left[\mathbf{i} + \frac{\mathbf{h}(\mathbf{hi})}{h^2}\right]\sin\beta\, d\beta\, r^2\, dr = \mathbf{v}_1' + \mathbf{v}_2' \quad (8)$$

where **T** is the Oseen tensor, **h** is the vector pointing from $P$ to $P'$, and $\beta$ is the polar angle between the vectors **r** and **s**. The vectors $\mathbf{v}_1'$ and $\mathbf{v}_2'$ represent the parts of **v'** corresponding to the first and second terms in brackets in the last integral of eq 8, respectively.

The integration over $\beta$ is readily performed by substitution from the law of cosines: $h^2 = s^2 + r^2 - 2rst$, where $t \equiv \cos\beta$. By assumption of a radially symmetric charge distribution about $O$, the $\beta$-dependent part of the integration of $\mathbf{v}_1'$ of eq 8 becomes

$$\int_0^\pi \frac{\sin\beta\, d\beta}{h} = \int_{-1}^{1}\frac{dt}{(s^2 + r^2 - 2srt)^{1/2}} \quad (9)$$

Evaluation of this integral leads to $2/s$ when $s > r$ and to $2/r$ when $s < r$.

Integration of the $\mathbf{v}_2'$ term over $\beta$ is complicated in the general case. For a polyion in Brownian motion the orientation of **h** with respect to the field direction **i** can be expected to be random. The device of preaveraging the Oseen tensor **T**, introduced by Kirkwood and Riseman,[21] then leads to $\mathbf{v}_2' = \mathbf{v}_1'/3$ as the result of this integration. Substitution of these results into eq 8 integrated over $\beta$ gives

$$\mathbf{v}' = \frac{X\mathbf{i}}{6\pi\eta}\left(\frac{1}{s}\int_a^s 4\pi\rho r^2\, dr + \int_s^\infty 4\pi\rho r\, dr\right) \quad (10)$$

Hermans[18] has previously obtained eq 10 for a different, but physically equivalent, model by a different method. The first integral in eq 10 represents $Q_s$, the charge of the ion atmosphere within a distance $s$ from $O$.

The integrals in eq 10 may be evaluated[26] by substitution of Poisson's equation, $\rho = -D\nabla^2\psi(r)/4\pi$, and replacement of $\nabla^2\psi(r)$ in the first integral by $(1/r^2)\, d/dr(r^2\, d\psi/dr)$ and in the second by $(1/r)[d^2(r\psi)/dr^2)$. The first integral gives

$$Q_s = \int_a^s 4\pi\rho r^2\, dr = D[a^2(d\psi/dr)_a - s^2(d\psi/dr)_s] \quad (11)$$

The second integral becomes

$$\int_s^\infty 4\pi\rho r\, dr = D\{s[d(\psi)/dr]_s + \psi_s\} \quad (12)$$

when $d(r\psi)/dr$ is taken to vanish at infinite $r$. Substitution of these results into eq 10 gives

$$\mathbf{v}' = \frac{DX\mathbf{i}}{6\pi\eta}\left[\frac{a^2}{s}\left(\frac{d\psi}{dr}\right)_a + \psi_s\right] = \frac{X\mathbf{i}}{6\pi\eta}\left(-\frac{Q_O}{s} + D\psi_s\right) \quad (13)$$

In the second form of eq 13 the *fixed* charge $Q_O$ on the site at (or surrounding) $O$ is expressed, with the use of eq 11, as

$$Q_O = -\lim_{s\to\infty} Q_s = Da^2(d\psi/dr)_a \quad (14)$$

where $s^2(d\psi/dr)_s$ is also taken to vanish at infinite $s$. The first equality of eq 14 simply states the charge neutrality of the overall system.

**Hydrodynamic Interaction Perturbations.** A perturbation of the solvent velocity will also be produced by the forces exerted by the particle on the fluid in consequence of its own motion. The convenient Burgers[27] procedure has often been employed for dealing with hydrodynamic interactions between different elements of the same particle. This procedure asserts that the velocity difference **v** − **U** between the fluid velocity **v** and the particle velocity **U** shall vanish (on the average) over the surface of contact. More particularly, for a particle possessing a long particle axis, this velocity difference is assumed to vanish over a cross section normal to the axis. The application of the Burgers procedure to wormlike cylindrical chains by Yamakawa and Fujii[3] will therefore be followed here, as will their notation for the most part.

The chain coordinate $p$ is taken to be the distance along the chain contour from one end of the chain. A distributed point force $\mathbf{f}(p)$ is assumed to be exerted on the solvent by the particle along the curving cylinder axis, such that

$$\int_0^L \mathbf{f}(p)\, dp = \langle\mathbf{F}\rangle = \mathbf{F}' = \sum_{k=1}^{Z} Q_k\mathbf{E}_0 \quad (15)$$

where $Q_k$ is the charge on site $k$, $Z$ is the number of such sites, $\langle\mathbf{F}\rangle$ is the mean frictional force exerted on the solvent by the particle, and **F'** is the force exerted on the particle by the external electric field, here taken to be simply that exerted on the site charges of the polyion by the applied field $\mathbf{E}_0$ (Hückel approximation). The velocity perturbation **v''** due to these forces at other points on the particle is then given, in the Yamakawa–Fujii treatment, at the normal cross section for axial point $p$, by

$$\mathbf{v}'' = \frac{1}{6\pi\eta}\int_0^L K(|p-q|)\langle\mathbf{f}(q)\rangle\, dq \quad (16)$$

$$K(|p-q|) = \langle|\mathbf{R} - \mathbf{r}|^{-1}\rangle \quad (17)$$

In eq 17 **R** represents the vector pointing from the position of $p$ to that of $q$, where $q$ represents any other point along the axis of chain contour, and **r** is the radius vector to the cylinder surface in the normal cross section at $p$. Equation 16 represents preaveraging of the Oseen tensor, where angle brackets indicate statistical averages at $p$ over the normal cross section *and* over all chain configurations. The Burgers criterion at each $p$ for this case is

$$\mathbf{v}_0 + \mathbf{v}' + \mathbf{v}'' - \mathbf{U} = 0 \quad (18)$$

where $\mathbf{v}_0$ is the unperturbed fluid velocity in the absence of the external electric field, which is taken here to be zero. If we make the obvious assumption, as for translational diffusion, that $\mathbf{U} = U\mathbf{i}$ is the same at all $p$, substitution of eqs 13 and 16 into eq 18 gives

$$\int_0^L K(|p-q|)\langle f(q)\rangle\, dq - X\sum_{k=1}^{Z} Q_k\langle|\mathbf{R} - \mathbf{r}|^{-1}\rangle_k + DX\sum_{k=1}^{Z}\langle\psi\rangle_k = 6\pi\eta U \quad (19)$$

where the mean force $\langle\mathbf{f}(q)\rangle$ is taken to be $\langle f(q)\rangle\mathbf{i}$ and $\langle\psi\rangle_k$ is the average value of the potential over the surface of the cross section at $p$ due to the charge at site $k$. The corresponding average $\langle s^{-1}\rangle_k$ of the reciprocal distance $s^{-1}$ in eq 13 from site $k$ to a point on the cylinder surface at this cross section has been set equal to $\langle|\mathbf{R} - \mathbf{r}|^{-1}\rangle_k$, where the latter has the same significance as $\langle|\mathbf{R} - \mathbf{r}|^{-1}\rangle$ when $q = q_k$, the axial point in the cross section containing site $k$.

Equation 19 may be solved approximately by the Kirkwood–Riseman procedure, which is most appropriate for long chains, as shown below. For shorter chains, or where a more exact solution of eq 19 is desired, the convenient numerical method of Schlitt[28] is preferable. Details of the application of this method are given in Appendix A.

**Kirkwood–Riseman Approximation.** The approximation of Kirkwood and Riseman[21] (KR) corresponds to $\langle f(q)\rangle$ = constant, independent of $q$. The integral equation may be solved in this case by a method similar to that used by Yamakawa and Fujii.[3] When eq 19 is multiplied by d$p$ followed by a further integration over $p$ from 0 to $L$, the result obtained, after inversion of summation and integration, may be written

$$2\langle f(p)\rangle \int_0^L (L-z)K(z)\,dz - X\sum_{k=1}^{Z} Q_k \int_0^L K(z_k)\,dz_k + DX\sum_{k=1}^{Z}\int_0^L \langle\psi\rangle_k\,dp = 6\pi\eta UL \quad (20)$$

where $z \equiv |p-q|$, $z_k \equiv |p-q_k|$, and the identity $\langle f(p)\rangle = \langle f(q)\rangle$ has been used. A similar approximation in eq 15 gives

$$\langle f(p)\rangle = \frac{X}{L}\sum_{k=1}^{Z} Q_k = \frac{QX}{L} \quad (21)$$

where $Q$ is the total charge on the polyion.

Substitution in eq 20 of $\langle f(p)\rangle$ from eq 21 and of the reduced mobility $u'$, as defined by eq 7, and specialization to the case that all $Q_k$ are identical and, with little loss of generality for chain polyions, equal to $\pm e$, leads to

$$\frac{2}{L}\int_0^L (L-z)K(z)\,dz - \frac{1}{Z}\sum_{k=1}^{Z} g(q_k) + \frac{D}{Q}\sum_{k=1}^{Z}\phi(q_k) = \frac{u'}{\xi} \quad (22)$$

$$g(q_k) \equiv \int_0^{q_k} K(z_k)\,dz_k + \int_0^{L-q_k} K(z_k)\,dz_k \quad (23)$$

$$\phi(q_k) \equiv \int_0^L \langle\psi\rangle_k\,dp = \int_0^{q_k}\langle\psi\rangle_k\,dz_k + \int_0^{L-q_k}\langle\psi\rangle_k\,dz_k \quad (24)$$

In eq 22 the familiar definition of the charge density parameter $\xi$ due to Manning[20]

$$\xi \equiv \frac{e|Q|}{DkTL} = \frac{e^2}{DkT}\frac{Z}{L} \quad (25)$$

has been inserted. It should be noted that $u'$ and $\xi$ are taken always to be positive and that the three algebraic terms on the left-hand side of eq 22 (with disregard of the minus sign before the second term) are all positive. The integrals $g(q_k)$ and $\phi(q_k)$ are taken with the site at $q_k$ as the origin of $z_k$.

In their treatment of the translational friction coefficient $\Xi$ of the wormlike chain in the KR approximation, Yamakawa and Fujii[3] set $\langle \mathbf{F}\rangle = \Xi\mathbf{U} = \Xi\mathbf{v}$. The above treatment reduces to this case, of course, since $\mathbf{v}'$ vanishes in the absence of an external electric field. Yamakawa and Fujii integrated the first term of eq 22, which is then equal to $6\pi\eta L/\Xi$, with the approximation to $K(z)$ given in their eq 37, which has also been used in the numerical calculations in this work. They computed the ratio $\Xi_\infty/\Xi$, where $\Xi_\infty$ represents the limiting value of $\Xi$ as $L \to \infty$, for various contour lengths $L$ and chain cylinder diameters $d'$. The results, presented as their Figure 7, were verified for representative cases in the course of this work by direct analytical integration, as well as by a numerical integration involving a 20-point Gaussian quadrature. The latter typically agreed within about 0.1% with the analytical result.

The simplification introduced by locating the discrete charge sites along the axial contour now appears, since $K(z_k) = K(z)$ for $z = z_k$. When the sum in the second term of eq 22 can be replaced by an integral, most suitably in the case of long chains, the first two terms cancel, and the KR approximation assumes a simple form, in terms of an average surface potential $\langle\psi_a\rangle$

$$\frac{u'}{\xi} = \frac{D}{Q}\sum_{k=1}^{Z}\phi(q_k) = \frac{D}{Q}\sum_{k=1}^{Z}\int_0^L \langle\psi\rangle_k\,dp = \frac{D\langle\psi_a\rangle L}{Q} \quad (26)$$

A similar cancellation occurs in other treatments of electrophoresis and leads to the usual proportionality between mobility and surface potential, as in eqs 1, 3, and 5. (See the Addendum for further discussion of this point.)

**Numerical Evaluation.** The theoretical results may be evaluated numerically when appropriate assumptions concerning the chain parameters and the form of the electrostatic potential are introduced. In cases where the chain can be characterized independently by hydrodynamic data, the reduced mobility $u'$ can be estimated without use of adjustable parameters. In this section the question of making such estimates is taken up on the basis of the preceding treatments: (1) the KR approximation, eq 22 or 26, and (2) the Schlitt solution: $u' = \xi/\phi_0$ given by eq A6 with $\phi_0$ evaluated with eq A16.

**(1) KR Approximation.** In performing numerical estimates of the extent of cancellation of the first two terms in eq 22, the integrals involving $K(z)$ and $K(z_k)$ were evaluated with use of eq 37 of Yamakawa and Fujii.[3] The parameters required for the use of this equation include the contour length $z$ between two axial points $p$ and $q$, the Kuhn length $A_K$ (equal to twice the persistence length), and the hydrodynamic radius $a$ used to represent the cylindrical cross section. Such parameters are available for hyaluronate from a previous study.[23] In that work estimates of the intrinsic viscosity (or limiting viscosity number) for the unperturbed chain were fitted to the wormlike cylinder model used here by means of the theoretical treatment of the same model given by Yamakawa and Fujii.[29] The values $A_K$ = 9.0 nm and $a$ = 0.55 nm provided the best fit when $Z$ was taken equal to 1.0$N$ (in nanometers), where $N$ is the number of repeating (disaccharide) units, so that $N = Z$ for the fully ionized polymer. This Kuhn length was consistent with the results of conformational modeling,[23,30] from which the value $A_K$ = 8.7 nm used in this work was derived. The results described here are quite insensitive to small variations in $A_K$. The value of $a$ is consistent with an estimate of 0.35 nm for the *unhydrated* radius from specific density increment (or small-angle X-ray scattering)[31] when allowance is made for a layer of water of hydration within the shear boundary. Examination of space-filling molecular models reveals, of course, that the wormlike cylinder is only a rough approximation to the molecular situation.

The $Z$ charge sites were placed along the axial contour at 1.0 nm spacing with the end charges at 0.5 nm from each chain end. When the integrations indicated in eqs 22 and 23 were performed analytically, the resulting expressions could be evaluated with the above parameters. The contribution to $u'/\xi$ of the first two terms in eq 22 ranged from −0.07 at $Z$ = 2 to −0.01 at $Z$ = 40 to −0.003 at $Z$ = 200, compared to typical experimental values of $u'/\xi$ between 2 and 6 (see Figure 2). These terms can clearly be neglected for long chains, as suggested in the simplification of eq 22 to eq 26. In any case the more

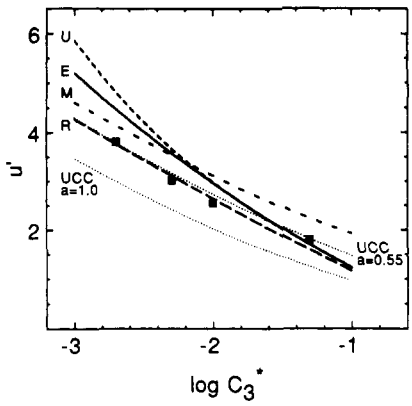


**Figure 2.** Theoretical results for the reduced electrophoretic mobility $u'$ plotted as a function of 1:1 electrolyte concentration $C_3^*$ for various model chains of infinite length and cylindrical radius $a = 0.55$ nm. Examples from this work are chains having uniformly spaced discrete axial charges at 1.0-nm separation: (U) the unperturbed wormlike chain (- - -, $A_K = 8.7$ nm); (E) the expanded frozen-worm chain (see text) (—, $A_K = 8.7$ nm); (R) the rigid-rod chain (– –, $A_K = \infty$). The theoretical result (*M*) of Manning (eq 37) for the bead model (- - -, $d = 1.0$ nm, $a_s = 0.55$ nm) is also shown, as are the uniformly charged cylinder (UCC) models (···) with $a = 0.55$ and 1.0 nm, as indicated. Experimental points (■) are those obtained for hyaluronate.[1]

accurate Schlitt solution, which includes the nearly canceling terms, reaches approximate convergence only at values of $Z$ higher than the preceding estimate would suggest and should be used for short chains.

Equation 26 will be shown below (see Discussion) to reduce readily to the results for the mobility $u'$ given by classic rodlike chain models with simple charge distributions. Numerical evaluation of $u'$ involves, in all cases, the problem of estimating the electrostatic (or $\zeta$) potential $\psi_a$ on the surface of the polyion. The difficulties encountered in the description of $\psi$ in the vicinity of a polyion are well-known, and many attempts have been made to find simple solutions of adequate accuracy to this problem. While this goal has not been achieved in the general case, the polyion of low linear charge density ($\xi < 1$), for which complete ionization of the counterions is approached, represents a particularly simple case.

In the use of a discrete-size conformational model to describe the potentiometric titration of hyaluronate,[4] a simple DH expression for the potential was found to provide good agreement with experiment for the low ionic strengths at which such an expression is approximately valid for simple 1:1 electrolytes. This agreement was found to occur, though somewhat fortuitously, even when the rodlike model with evenly spaced sites was used to represent the polyion.

The use of this potential function in the present case, as well, therefore appears to be justified. When the value of $\psi$ at a given point in the solution is taken to be a sum of the independent contributions from each of the sites $k$ of a single polyion, and the conformationally averaged contribution from a single site is written

$$\langle\psi\rangle_k = \frac{Q_k}{D}\left\langle\frac{\exp(-\kappa s)}{s}\right\rangle_k \tag{27}$$

substitution of eq 27 into eq 26 leads to

$$\frac{u'}{\xi} \equiv \frac{1}{Z}\sum_{k=1}^{Z}\int_0^L\left\langle\frac{\exp[-\kappa(|\mathbf{R}-\mathbf{r}|)]}{|\mathbf{R}-\mathbf{r}|}\right\rangle_k dp \tag{28}$$

Equation 28 may be evaluated by a numerical method at each site $k$ by splitting the integral into two terms with limits, as in eq 24. The sum divided by $Z$ clearly represents an average of this integral over all the sites. In the long-chain limit being considered here, each site will contribute equally and a single integration suffices:

$$\lim_{L\to\infty} u' = 2\xi\int_0^\infty\left\langle\frac{\exp[-\kappa(|\mathbf{R}-\mathbf{r}|)]}{|\mathbf{R}-\mathbf{r}|}\right\rangle_k dp \tag{29}$$

The factor of 2 appears because the site $k$ can be regarded in this case as located at the center of a chain stretching from $-L/2$ to $L/2$.

The average occurring in eqs 27–29 has been considered for the hyaluronate ion in a theoretical calculation[4] of the electrostatic free energy, for which the distance $r_{jk}$ between charged sites $j$ and $k$ was involved. While the averaging should in principle be done over all conformational states, an approximation to the electrostatic free energy in that work used a rigid model which reproduced rather well the results of a more accurate conformational calculation employing the Monte Carlo technique. This model, termed the "frozen-worm approximation", used an expansion correction to the unperturbed root-mean-square end-to-end distance to derive values of $r_{jk}$, which were used as *fixed* distances to replace the conformational average of the kind appearing in eq 29. The assumption that similarly good agreement can be expected in the present calculation seems reasonable.

Fixed values of the distance have therefore been estimated from $|\mathbf{R}-\mathbf{r}| = (\alpha_R^2\langle R^2\rangle_0 + a^2)^{1/2}$, where $\alpha_R$ is the expansion factor calculated previously,[4] and $\langle R^2\rangle_0$ is the unperturbed mean-square end-to-end distance for the wormlike chain of contour length $z_k$. Negligible errors can be expected from the assumption of orthogonality of $\mathbf{R}$ and $\mathbf{r}$ implicit in this estimate. Numerical values of all distances were calculated in dimensionless units as multiples of the Kuhn length $A_K$. Substitution of the resulting values of $|\mathbf{R}-\mathbf{r}|$ into eq 29 as fixed distances to replace the conformational average then permitted the indicated integration by a numerical method. The latter was carried out by 80-point Gaussian quadrature with use of tabulated numerical coefficients.[32]

**(2) Schlitt Solution.** The numerical evaluation of the $\phi_j$, and especially $\phi_0 = u'/\xi$, can be carried out by substitution of the coefficients $K_{ij}$, $K_{ik}$, and $\langle\psi\rangle_{ik}$, estimated as for the continuous case, into eqs A10 and A14. Solution of the resulting linear set may then be carried out by the matrix inversion indicated by eq A16. The locations of sites $i$ and $j$ along the axial contour were chosen as the Gaussian quadrature abscissae, and charge sites $k$ were chosen as indicated above for the KR approximation case.

## Results

Computed values of the long-chain limit (KR approximation) to $u'$ are plotted in Figure 2 as a function of $C_3^*$, the molar concentration of 1:1 electrolyte (equal to the ionic strength $I$) at infinite dilution of polymer. This notation is consistent with previous usage for this system,[2] where component 1 denoted solvent water, component 2 the polymeric electrolyte (polyion plus counterions), and component 3 the electrolyte component of low molecular weight. Values of $C_3^*$ are related to $\kappa$ (in nm$^{-1}$) at 25 °C by $\kappa = 3.29C_3^{*1/2}$ at $C_2 = 0$. The hyaluronate polyion is taken to have charge spacings $d \equiv L/Z$ along the chain contour of 1.0 nm when fully ionized, so that $\xi = 0.716/d$ (with $d$ in nanometers) = 0.716 at 25 °C, when the value $D = 78.3$ for water is inserted in eq 25.

Results are shown in Figure 2 for the discrete-site cylinder model of hyaluronate ($a = 0.55$ nm) described above for three different chain types: (1) the *expanded*

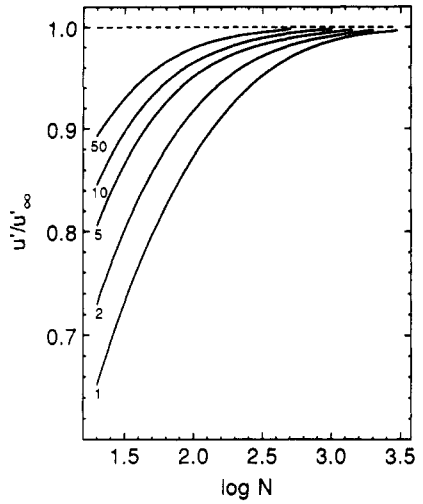


**Figure 3.** Reduced electrophoretic mobility of chains of $N$ disaccharide subunits as a fraction $u'/u'_\infty$ of that of the chain of infinite $N$. Data are for the fully ionized ($N = Z$) unperturbed wormlike chain of Figure 2, as calculated by the Schlitt integration procedure. Values of $10^3$ $C_3$* are indicated for each curve.

(frozen-worm) conformation ($A_K$ = 8.7 nm, curve E); (2) the *unperturbed* wormlike conformation ($A_K$ = 8.7 nm, curve U); and (3) the long-rod model (infinite $A_K$, curve R). The latter corresponds, with respect to the location of charges, to a polyion model used by Manning,[33] which consisted of uniformly spaced discrete charges along a straight line.

The result for the long-rod model can be verified by direct integration. In deriving the potential of the continuous line of charge, Manning[11] showed that the integral appearing in eq 26 gives $2K_0(\kappa a)$, where $K_0(\kappa a)$ is the modified Bessel function of the second kind of order zero, so that

$$u' = 2\xi K_0(\kappa a) \tag{30}$$

Values of $u'$ calculated from $K_0(\kappa a)$ (ref 32, p 379) reproduce precisely those obtained by Gaussian quadrature.

The dotted lines in Figure 2 show the similar result for the cylinder of uniform surface charge (UCC), when the DH approximation[13,34] to $y_0$ (eq 32) is used in eq 6 (with $f$ = 1). Inclusion of the UCC model of radius $a$ = 1.0 nm shows the reduced mobility predicted for the radius which provided the best fit to potentiometric titration data for hyaluronate.[2]

In addition to dependence of the mobility on the ionic strength, the solutions to eqs A10 and A14 by the Schlitt procedure provide predictions concerning the dependence on chain length, as expressed by the number $Z$ of charge sites. The results of these calculations, which are shown in Figure 3, extrapolate to the KR approximation as $Z$ becomes large. As would be expected, the approach to this limit occurs at higher $Z$ as the ionic strength decreases.

## Discussion

Results in the preceding section were based on a wormlike cylinder model with discrete axial sites. The special case of the infinite long-rod (or straight-cylinder) model can be readily adapted to other simple charge distributions, which will be discussed in the next section.

**(I) Long-Rod Model. (a) Axial Charge Distributions.** For uniformly spaced discrete axial sites, the potential $\psi_a$ on the cylinder surface varies in a cyclical fashion along the chain contour, its absolute value being largest in the plane containing a charge site and smallest in that midway between two sites. When the polyion charge is subdivided into smaller, but equal, parts, the result for $u'$, eq 30 (KR approximation), will remain unchanged. The limit of such subdivision, i.e., the line charge having a continuous distribution of uniform density, will thus also give this result.

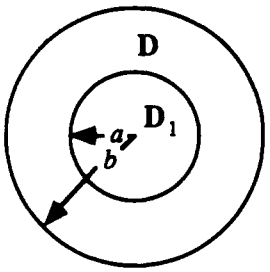


**Figure 4.** Dielectric cylinder having a core ($r < a$) of dielectric constant $D_1$ surrounded by the annular shell ($b > r > a$) of bulk dielectric constant $D$, where $b$ represents the minimum radius of penetration of centers of counterions in the original model of Gorin[13] and Hill.[34]

It may be instructive to obtain eq 30 in a slightly different way. For any distribution that leads to a *uniform* potential $\psi_a$ on the cylinder surface, $u'/\xi$ can be obtained by integrating eq 26 to give

$$u' = D\psi_a L\xi/Q = y_0 \tag{31}$$

where the definition of $\xi$ (eq 25) has been used. Equation 31 is identical with eq 6, the result of Schellman and Stigter[14] when $h(x_0) = 1$, hence $f = 1$, where $x_0 \equiv \kappa a$. The numerical value of $\psi_a$ to be used will, of course, depend on the electrostatic model chosen and assumptions concerning the location of the surface. Insertion of the continuous line-charge potential $|\psi_a| = 2eK_0(x_0)/Dd$, as given by Manning,[11] into $y_0$ reduces eq 31 to eq 30.

**(b) Surface Charge Distributions.** The models employed in the theoretical treatment have used the DH "limiting law" assumptions that the fixed axial sites of the polyion cylinder are point charges immersed in a structureless (continuum) electrolyte medium with spherical symmetry of charge about each site. The radius $a$ was introduced to define a cylindrical surface of shear. Examination of molecular models of hyaluronate and most other polyions makes clear that a more realistic model would place the charge sites at or near the surface of the polyion. The contact with solvent of the carboxylate group in hyaluronate presumably resembles that in a small anion, such as acetate. In addition, the organic material of the polyion will influence the electrostatic potential in its vicinity, through both its low dielectric constant and its exclusion of the small ions in the solvent.

Theoretical investigations of these effects in aqueous solution have often employed the dielectric (straight) cylinder model having the cross section shown in Figure 4, where a uniform low dielectric constant $D_1$ at $r < a$ changes abruptly to the uniform high dielectric constant $D$ of the solvent at $r > a$. A charge-free annular region ($b > r > a$) has sometimes been included to allow for the exclusion of the centers of small ions from that region.

The assumption of a radially symmetric charge distribution about the polyion charge sites used to obtain eq 13, and thus eqs 22 and 26, is unrealistic when the sites are placed on the surface of such a cylinder. The continued use of eq 26 can be tentatively justified by appeal to the classical theory of colloid electrophoresis,[7,12] where the crucial parameter is the $\zeta$ potential, defined as the electrostatic potential at the surface of shear of a moving particle and thus corresponding to the surface potential $\psi_a$ used in this work.

The hydrodynamic analysis of Henry, which neglected relaxation effects, involved a complete solution of the Navier–Stokes equation for the dielectric cylinder of Figure 4 with a uniform surface charge at $r = a = b$ and a continuum solvent ($r > a$). Henry's result for this cylindrically symmetric case, taken with the averaging procedure of Schellman and Stigter, gives eq 31 for $x_0 \ll 1$. This agreement, when they can be compared, of eq 26 for the discrete axial distribution with Henry's analysis for the UCC suggests that eq 26 should provide a reasonable approximation for the dielectric cylinder with discrete sites on the surface, as well.

Skolnick and Fixman[35] obtained a solution in the DH approximation for the potential of a *discrete* point charge placed on the surface of an infinite dielectric cylinder ($r = a = b$). In this case $\psi_k$ varies both with the azimuthal angle $\gamma$ (measured from $\gamma = 0$ at the charge site) and the axial distance $z_k$ from the charge site. As shown in Appendix B, integration of their result over the surface of the cylinder to obtain $\phi(q_k)$ according to eq 24 leads to eq B7. When the sum indicated in eq 26 is performed, the *location* of individual sites on the surface is immaterial, provided that the potential can be regarded as a superposition of the single-site potentials of Skolnick and Fixman, which is consistent with the DH approximation.

An obvious consequence of this argument is that the value of $u'$ for the long-rod cylinder having a *uniform* surface charge on $r = a = b$ (the UCC model) is also given by eq B7 when the surface charge is considered as a superposition of infinitesimal charge elements. The assumption for surface sites of the KR approximation of eq 26, taken with the Skolnick–Fixman solution for the potential, is therefore *equivalent* to the result obtained for this model[14] by insertion of the solution[13,34] for the UCC surface potential into eq 6 (with $f$ set equal to unity).

$$u' = y_0 = 2\xi \frac{K_0(x_0)}{x_0 K_1(x_0)} \tag{32}$$

In the case of varying potential on the shear surface, the parameter $y_0$ is therefore redefined by

$$y_0 \equiv |\langle \psi_a \rangle| e/kT \tag{33}$$

with $\langle \psi_a \rangle$ defined by the last equality of eq 26. The curves marked UCC in Figure 2 represent plots of eq 32 for two different values of $a$. Since the function $x_0 K_1(x_0)$ deviates from unity by no more than 5% for $x_0 < 0.2$ or 15% for $x_0 < 0.4$ ($C_3^* < 0.01$ or 0.05 M, respectively, when $a = 0.55$ nm), the effect on $u'$ of placing the charge on the cylinder surface rather than axially is relatively small in the long-rod case, especially at low ionic strength. The effect of the value chosen for the radius of shear $a$ is, however, clearly significant.

**(c) Finite Ion Size.** A traditional way of dealing with volume exclusion effects of small ions has been to introduce a charge-free region $b > r > a$ in Figure 4 into which the centers of the small ions do not penetrate. When the assumption of Gorin is made that the surface of shear remains at $r = a$, the reduced potential there, now termed $y_{0i}$, becomes[13,34]

$$y_{0i} = 2\xi \left[ \frac{K_0(x_b)}{x_b K_1(x_b)} + \ln \frac{b}{a} \right] = f_i y_0 \tag{34}$$

where $x_b \equiv \kappa b$ and the factor $f_i$ provides a correction to eq 32 for this effect. Equation 34 does not depend on the location of the charge within the cylinder, provided only that the charge distribution is cylindrically symmetric. Thus, even the axial line of charge gives this result when exclusion effects of the type indicated by Figure 4 are included.

**Table I**
**Correction Factor $f_i$ for Finite Ion Size**

| $C_3^*$ | $x_0$[a] | $r_i$, nm | $f_i$ 0.20 | $f_i$ 0.40 |
|---|---|---|---|---|
| 0.001 | 0.057 | | 1.004 | 1.008 |
| 0.002 | 0.081 | | 1.007 | 1.014 |
| 0.005 | 0.128 | | 1.014 | 1.028 |
| 0.010 | 0.181 | | 1.023 | 1.046 |
| 0.025 | 0.286 | | 1.045 | 1.088 |
| 0.050 | 0.405 | | 1.073 | 1.119 |
| 0.100 | 0.572 | | 1.116 | 1.221 |

[a] Polyion radius of shear $a = 0.55$ nm.

Although Skolnick and Fixman did not solve the potential problem of the point charge with the charge-free layer between $a$ and $b$, the results of Bailey,[36] who studied the dielectric cylinder of Figure 4 with $b > a$ for a helical array of discrete surface charge sites, strongly suggest that eq 34 will result in that case when the potential is averaged over the surface at $r = a$.

The numerical effect of the use of eq 34 rather than eq 32 is shown in Table I for the value $a = 0.55$ nm chosen for hyaluronate and two different choices of the small ion radius, $r_i \equiv b - a$. The choice $r_i = 0.2$–$0.25$ nm corresponds to a typical choice[37a] for alkali-metal and alkaline-earth halides in fitting data for activity coefficients to the DH theory. The larger ions ($Tris^+$ and $acetate^-$) used in the electrophoresis experiments[1] might be expected to have values of $r_i$ as large as 0.3–0.4 nm. The correction factors $f_i$ listed in Table I are the ratios of eq 34 to eq 32 at a selection of ionic strengths $C_3^*$. The corrections are smaller than 5% for $C_3^* < 0.01$ but become increasingly significant at higher ionic strengths, where the DH potential itself is less reliable.

Since molecular modeling of hyaluronate suggests that a monolayer of water lies within the shear surface, the counterions may well penetrate this layer to some extent. In this case $b - a$ will be smaller than $r_i$ and may even vanish. The size of the correction is therefore open to question, and no such corrections have been made in comparisons with experiment.

**(d) Ion-Atmosphere Relaxation. Nonlinearity of the PB Equation.** While the long-rod models might appear to provide better agreement with experimental data for hyaluronate than the wormlike models, as judged by Figure 2, it must be recalled that two important effects have been neglected in the preceding treatment: (1) the relaxation effect of the ionic atmosphere in electrophoretic transport and (2) the effects of deviations from the Debye–Hückel approximation to the potential. As mentioned previously, Stigter has provided[38] numerical solutions to the nonlinear PB equation for the long-rod cylinder with $a = b$. A comparison in Table II for the long-rod model of hyaluronate shows that his values of $y_0 \equiv y_{0(S)}$ are smaller than $y_{0(DH)}$ by at most about 9% at $x_0$ values of interest.

Numerical estimates of the relaxation correction factor $f$ of eq 6 were tabulated[39] by Stigter for the randomly oriented UCC model as a function of $y_{0(S)}$ and $x_0$. Further parameters were the reduced friction factors $m_\pm$ for the small ions of the supporting 1:1 electrolyte. The values of $f_S$ given in Table II were estimated from these tabulations for the experimental conditions of the mobility measurements[1] in Tris acetate buffers of varying concentration. The limiting molar conductivity values at 25 °C in units of S $cm^2$ $mol^{-1}$ were taken to be $\Lambda_+^0 = 29.7$ for Tris[40] and $\Lambda_-^0 = 40.9$ for acetate.[37b] Corrections were made

**Table II**
**Estimated Relaxation Correction Factor $f$ in $u' = fy_0$ for Hyaluronate[a]**

| | | model | | | | | | |
|---|---|---|---|---|---|---|---|---|
| | | UCC[b] | | | EA[c] | | Manning[d] | |
| $C_3^*$ | $x_0$ | $y_{0(DH)}$ | $y_{0(S)}$ | $f_S$ | $y_{0(S)}$ | $f_S$ | $y_{0(M)}$ | $f_M$ |
| 0.001 | 0.057 | 4.29 | 3.92 | 0.88 | 4.43 | 0.86 | 4.62 | 0.70 |
| 0.002 | 0.081 | 3.81 | 3.48 | 0.90 | 3.98 | 0.87 | 4.15 | 0.72 |
| 0.005 | 0.128 | 3.20 | 2.95 | 0.91 | 3.25 | 0.90 | 3.55 | 0.74 |
| 0.010 | 0.181 | 2.75 | 2.55 | 0.93 | 2.74 | 0.92 | 3.12 | 0.76 |
| 0.025 | 0.286 | 2.20 | 2.08 | 0.95 | 2.08 | 0.95 | 2.60 | 0.78 |
| 0.050 | 0.405 | 1.81 | 1.73 | 0.97 | 1.61 | 0.98 | 2.24 | 0.79 |
| 0.100 | 0.572 | 1.47 | 1.42 | 0.98 | 1.20 | 1.00 | 1.93 | 0.80 |

[a] The cylinder radius in all numerical calculations is 0.55 nm; $d$ = 1.0 nm; electrolyte is Tris acetate. [b] Uniformly charged cylinder (UCC) model: $y_{0(DH)}$ calculated from eq 32, $y_{0(S)}$ and $f_S$ as described in text. [c] Expanded wormlike cylinder, axial charge sites (EA) model: $y_{0(DH)}$ (not shown) as for curve $E$ in Figure 2, $y_{0(S)}$ and $f_S$ as described in text. [d] Manning discrete-site model:[20] $y_{0(M)} = u'$ from eq 37, $a_s$ = 0.55 nm; $f_M$ calculated as described in text.

to these values for concentration effects on $\Lambda_\pm$. Some extrapolation was required when these estimates were made, since the values of $m_\pm = 12.86/\Lambda_\pm$ at 25 °C for these ions are somewhat higher than those given in Stigter's tabulations.

**(II) Wormlike Model.** Since this model generally provides a better description of the conformational behavior of chain molecules, its use is to be preferred in the treatment of physical properties when the latter involve interactions at distances of the order of a persistence length or greater along the chain contour. The reduced mobility $u'$ for this model has been treated in the theoretical section for the case where the charge sites are located along the contour axis of the chain. Since $u'$ for the long-rod model changes only slightly when surface charge distributions are used instead, we can reasonably expect that the wormlike model will change similarly.

In the estimation of values of $u'$ for the expanded wormlike model, the *ratio* of the value for surface sites to that for axial sites at a given $x_0$ has been assumed equal to that for the corresponding rodlike model when the two models have the same value of $u'$ (or average surface potential) for axial sites.

**Manning Theory.** An earlier theory of electrophoretic mobility of chain molecules bearing discrete charge sites was that of Manning.[20] Instead of the wormlike cylinder model used here, Manning's theory employed the hydrodynamic model of Kirkwood,[22] which regards the polymer chain as a sequence of structural units, each of which is taken as a point source of friction. This model was first used by Kirkwood and Riseman[21] in their theory of the polymer friction coefficient. The result obtained by Manning in the Debye–Hückel approximation, when relaxation effects were neglected, may be written in our notation by combining Manning's (M) eqs M2, M5, and M10 with $Q = Ne$ to give

$$u' = \frac{6\pi\eta\xi d}{\zeta} + \xi d \sum_{i=1}^{N}\sum_{j=1}^{N} \langle r_{ij}^{-1} e^{-\kappa r_{ij}} \rangle \qquad (35)$$

where $d \equiv L/Z$. For the linear polyion model used by Manning with equal spacing $d$ between charge sites, the double sum gives $-(2N/d)\ \ln\ [1 - \exp(-\kappa d)]$ and eq 35 becomes

$$u' = \frac{6\pi\eta\xi d}{\zeta} - 2\xi \ln\ [1 - \exp(-\kappa d)] \qquad (36)$$

The friction coefficient $\zeta$ represents the frictional resistance that would result if the chain were cut into its individual units and would then be completely analogous to that appearing in the conductivity theory for small ions. Robinson and Stokes[37c] have shown that Stokes' law in the form $\zeta = 6\pi\eta a_s$ provides a good fit to experimental conductivity data for the tetraalkylammonium cations when the radius $a_s$ is calculated for the assumed spherical ions from the molal volumes, provided $a_s > 0.5$ nm. Introduction into eq 36 of Flory's suggested use[41] of this expression for $\zeta$ in the context of the structural unit, assumed spherical, of the chain model leads to

$$u' = 2\xi\{d/2a_s - \ln\ [1 - \exp(-\kappa d)]\} \qquad (37)$$

Manning[20] considered only the case $\kappa d \ll 1$ to obtain $u_M' = -2\xi \ln (\kappa d)$ for univalent charge sites, which follows from eq 37 with neglect of the first term in braces and retention of the first noncanceling term from the expansion of the exponential. For cases of interest here, this approximation is not valid, and the full eq 37 should be used instead.

The curve marked M in Figure 2 represents a plot of eq 37 with $a_s = a$ = 0.55 nm and $d$ = 1.0 nm, as for the other curves. While the value of $u'$ given by this model lies about 10% higher than those of the other long-rod models at $C_3^* = 10^{-3}$ M, the use of the *constant* first term in eq 37 leads to significantly higher values at the larger ionic strengths.

Manning provided estimates of relaxation effects as a part of his theoretical treatment of mobility. The corrections given in Table II as $f_M$ for the Manning model have been calculated from eq 38 of ref 20 ($f_M$ is the reciprocal of Manning's $\beta$) with use of the same conductivity data. The relaxation corrections of Manning, which use a DH potential expression, deviate considerably more than unity than do those of Stigter.

**Comparison of Calculated $u'$ with Experiment. (a) Hyaluronate ($\xi < 1$).** Calculated theoretical values of $u'$ for hyaluronate, which include the relaxation and nonlinear PB corrections of Table II, are shown in Figure 5 for several models of interest. Corrections for finite counterion size have not been included because of their uncertain validity, as mentioned above. If made, they would raise calculated $u'$ values by the factor $f_i$ (eq 34 and Table I), in addition to a small further increase due to somewhat smaller relaxation effects as the ion atmosphere

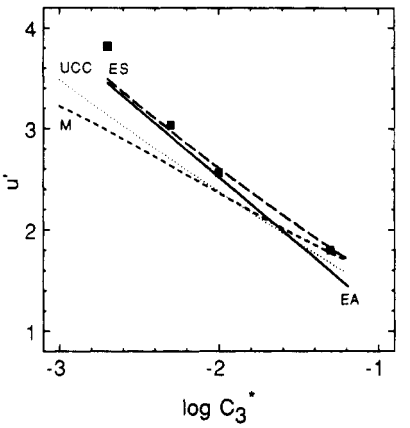


**Figure 5.** Theoretical reduced electrophoretic mobility $u'$ of hyaluronate ($\xi$ = 0.716) corrected for effects of nonlinearity of the Poisson–Boltzmann potential and ion-atmosphere relaxation as described in the text. Chain models and designations correspond to those in Figure 2 except that EA (—) is used to designate axial charge sites and ES (– –) surface charge sites for the expanded frozen-worm chain. The Manning chain $M$ is corrected only for relaxation effects. All chains have radius $a$ = 0.55 nm. The experimental points are the same as those of Figure 2.

**Table III**
**Estimated Relaxation Correction Factor $f$ in $u' = fy_0$ for $\xi = 1.43$[a]**

| | | model | | | | | | |
|---|---|---|---|---|---|---|---|---|
| | | UCC[b] | | | EA[c] | | Manning[d] | |
| $C_3$* | $x_0$ | $y_{0(DH)}$ | $y_{0(S)}$ | $f_S$ | $y_{0(S)}$ | $f_S$ | $y_{0(M)}$ | $f_M$ |
| 0.001 | 0.057 | 8.58 | 6.32 | 0.81 | 6.81 | 0.80 | 6.87 | 0.67 |
| 0.002 | 0.081 | 7.63 | 5.69 | 0.83 | 6.24 | 0.83 | 6.20 | 0.69 |
| 0.005 | 0.128 | 6.40 | 4.91 | 0.85 | 5.27 | 0.84 | 5.33 | 0.72 |
| 0.010 | 0.181 | 5.50 | 4.33 | 0.86 | 4.56 | 0.85 | 4.68 | 0.74 |
| 0.025 | 0.286 | 4.40 | 3.59 | 0.89 | 3.61 | 0.89 | 3.86 | 0.77 |
| 0.050 | 0.405 | 3.63 | 3.06 | 0.91 | 2.91 | 0.92 | 3.27 | 0.79 |
| 0.100 | 0.572 | 2.94 | 2.56 | 0.94 | 2.22 | 0.95 | 2.71 | 0.81 |

[a] The cylinder radius in all numerical calculations is 0.55 nm; $d$ = 0.5 nm; electrolyte is NaCl. [b] Uniformly charged cylinder (UCC) model: $y_{0(DH)}$ calculated from eq 32, $y_{0(S)}$ and $f_S$ as described in text. [c] Expanded wormlike cylinder, axial charge sites (EA) model: $y_{0(DH)}$ (not shown) 2× curve $E$ in Figure 2, $y_{0(S)}$ and $f_S$ as described in text. [d] Manning discrete-site model:[20] $y_{0(M)} = u'$ from eq 37, $a_s$ = 0.55 nm; $f_M$ calculated as described in text.

is moved away from the polyion cylinder. Such corrections would depend on the value chosen for $r_i$, but should in any case be quite small at $C_3$* < 0.01 M.

The most striking result of Figure 5 is the similarity of the predicted values of $u'$ for the different models. Over the range of $C_3$* values of experimental interest they differ by a maximum of about 20%. The fit to the experimental data for hyaluronate is quite satisfactory and appears to be slightly better for the wormlike models.

As mentioned previously, the choice of the cylinder radius $a$ = 0.55 nm was based on a fit[23] of the Yamakawa–Fuji wormlike model[29,42] to intrinsic viscosity data for hyaluronate. Actually, only data for oligosaccharides are decisive in this respect, because only at molecular weights less than about $10^4$ are calculated values of $[\eta]_0$, the unperturbed intrinsic viscosity, sufficiently sensitive to the value of chain radius chosen and sufficiently insensitive to the choice of the Kuhn length. A re-examination of that calculation suggests a best fit of $a$ to be 0.53 (±0.05) nm. The effect of use of the lower (upper) suggested limit of $a$ on calculated values of $u'$ of Figure 2 (for $a$ = 0.55 nm) is to increase (decrease) $u'$ by from 4 (2)% at $C_3$* = $10^{-3}$ M to 9 (3)% at $C_3$* = 0.1 M for the wormlike or rodlike surface-site models and slightly more for the axial-site models, so that the error limits of $u'$ due to probable uncertainties in $a$ are also relatively small.

Perhaps more important in this respect are errors in the calculated values of $[\eta]_0$[29] due to neglect of fluctuations in hydrodynamic interactions implicit in the preaveraging of the Oseen tensor. Dynamic simulations of polymer motion with fluctuating hydrodynamic interactions[43] suggest that $[\eta]_0$ may be significantly overestimated (and hence our values of $a$ underestimated) due to this effect. The probable magnitude of this error is not clear.

**(b) Singly Charged Monosaccharides ($\xi > 1$).** Ionized polysaccharides that have one or more charge sites per *mono*saccharide have values of $\xi > 1$ and therefore lie in the region of "counterion condensation", where the *calculated* $\xi$ is replaced by an *effective* value of unity, according to the Manning theory of polyelectrolytes.[11] In the present work the preference has been rather to determine effects of the electrostatic potential on the spatial distribution of the small ions in the solvent by use in all cases of the Poisson–Boltzmann equation and with the value of $\xi$ given by eq 25. Calculations for the case when the average charge spacing projected on the axial contour is $d$ = 0.50 nm ($\xi$ = 1.43) are presented in Table III and Figure 6. In the absence of hydrodynamic data for

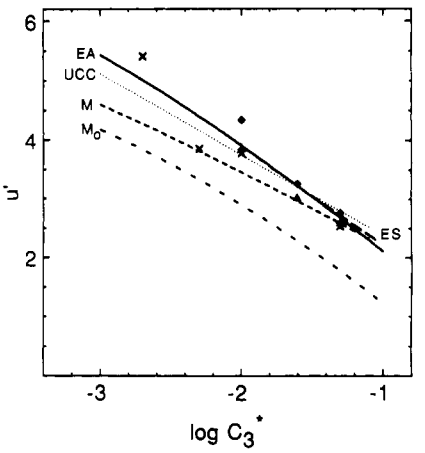


**Figure 6.** Theoretical reduced electrophoretic mobility $u'$ of polysaccharides having one charge per monosaccharide ($\xi$ = 1.43) for the chain models and with the corrections of Figure 5. The expanded chains are assumed to have the same expansion factors as for hyaluronate. The Manning models represented are $M$, calculated from the complete eq 37, and, for comparison, $M_0$, which represents the result originally suggested by Manning (eq 35 of ref 20) for $\kappa d \ll 1$. For these models the Manning assumption $\xi$ = 1 and relaxation effects are included. The experimental points are for chondroitin 4-sulfate[1] (×, sample CS-8-T, see text), sodium polygalacturonate[44] (◆), and sodium alginate[44] (▲).

such polymers the Kuhn length $A_K$, the radius $a$, and expansion effects have been assumed to be the same for chains EA and ES as for hyaluronate. Calculated mobilities are rather insensitive to the choice of $A_K$, and structural similarities of the hexuronic acid subunits should result in similar $a$ values, although the bulky $SO_4^-$ on the *N*-acetylhexosamine ring of chondroitin 4-sulfate may lead to a higher $a$ value in that case. Expansion effects will undoubtedly be somewhat larger than for hyaluronate, so that the calculated mobilities are likely to be slightly too large at $I = C_3$* < 0.01, where the expanded models differ significantly from the unperturbed chain (see Figure 2).

The reduced mobilities for this case for the Manning model are represented in Figure 6 by curve M, calculated from eq 37 with $\xi$ set equal to 1, and curve $M_0$, from $u_M' = -2 \ln (\kappa d)$, which is the original Manning suggestion (eq 36 of ref 20), both corrected for relaxation effects by multiplying by Manning's $\beta^{-1} \equiv f_M$. The experimental points in Figure 6 represent the data of Tuffile and Ander[44] for sodium polygalacturonate and sodium alginate, both of which have ionized hexuronic acids in all monosaccharide subunits, and data for chondroitin sulfate,[1] corrected by the factors appropriate for its molecular mass ($N$ = 60) from Figure 3. The fit of the models to experimental data is similar in character to that for hyaluronate and typically within experimental error for the UCC and expanded wormlike cylinder models, except perhaps at the lowest ionic strength. The deviation of curve $M_0$ from curve M clearly indicates that the condition $\kappa d \ll 1$ is far from satisfied here.

**Relation of Electrophoretic Mobility to Potentiometric Titration.** Models that assume a uniform surface potential $\psi_a$ provide a ready description of potentiometric titration because of the relation of $\psi_a$ to the electrostatic free energy. The relation usually invoked for polyacids is[45]

$$\Delta pK \equiv pK' - pK_0' = 0.4343 y_0 \quad (38)$$

$$pK' \equiv pH + \log [(1-\alpha)/\alpha] = pK_0' + m\alpha \quad (39)$$

where the last equality of eq 39 assumes a linear plot of

Table IV
Experimental and Calculated Values of $u'/2.303m$ for Hyaluronate

| | | | $u'/2.303m$ | |
|---|---|---|---|---|
| $C_3$* | $u'$ [a] | $m$ [b] | exptl | calcd [b] |
| 0.001 | | 1.30 | | |
| 0.002 | 3.83 | (1.12) | 1.48 | 1.36 |
| 0.005 | 3.04 | (0.91) | 1.45 | 1.38 |
| 0.010 | 2.57 | 0.77 | 1.45 | 1.43 |
| 0.025 | (1.88) | 0.55 | 1.48 | |
| 0.050 | 1.80 | (0.51) | 1.53 | 1.63 |
| 0.100 | (1.63) | 0.43 | 1.65 | 1.72 |

[a] Values in parentheses are interpolated from quadratic least-squares fits of experimental values of $u'$[1] and of $m$[2]. [b] Calculated values are for the expanded-worm model, DH potential (axial sites with $a$ = 0.55 nm for $u'$; Monte Carlo calculations[4] for $m$) without corrections.

p$K'$ against the degree of ionization $\alpha$ having a slope $m$. Such plots are obtained from potentiometric titration[2] of hyaluronic acid at constant $C_3$*, the 1:1 electrolyte concentration in the solvent at dialysis equilibrium. Values of $m$ were fitted rather accurately as a function of $C_3$* by use of eq 32 for $y_0$ at a cylinder radius $a$ = 1.0 nm. A slightly better fit was obtained[2] for the same $a$ value with the numerical solution[38] for $y_0$ from the nonlinear Poisson–Boltzmann equation.

Combination of eqs 6, 38, and 39 at $\alpha$ = 1 yields

$$u' = 2.303mf \tag{40}$$

The values of $u'/2.303m$ found experimentally for hyaluronate, which are shown in Table IV, lie about 50% above that predicted by eq 40: $u'/2.303m = f$, even when $f$ (typically less than unity) is set equal to 1.[1] This effect can also be seen in Figure 2, where the experimental values of $u'$ are seen to lie well above the predictions of the model (curve UCC, $a$ = 1.0 nm), although they are fitted rather well by curve UCC, $a$ = 0.55 nm. The UCC model clearly does *not* provide a consistent account of the results of these two experimental techniques.

The discrete-site (DS) models provide much better agreement with experiment in this respect. In Table IV are shown theoretical values (DH potential) of $u'$ from this work and $m$ from previous work[4] for the frozen-worm approximation. Corrections to these values have not been made for relaxation effects (on $u'$) or the Skolnick–Fixman[35] effect (on $m$), which tend to compensate each other in the calculated ratios $u'/m$. Similarly, neglect of the effects of nonlinearity and assumptions made about chain conformation, while they affect the predicted individual properties $u'$ and $m$, have little influence on this ratio because $u'$ and $m$ are separately proportional to the electrostatic potential.

In view of the clear superiority of the discrete-site model in accounting for the relation of these two properties, the question arises why the UCC model fails in this respect. Examination of Figures 5 and 6 suggests that, given information about the correct cylinder radius to use from a fit to hydrodynamic data of the wormlike cylinder model, the UCC model provides a correct account of electrophoretic mobility. As mentioned earlier, however, a much larger cylinder radius must be used to provide a correspondingly good fit to data from potentiometric titration. The error therefore appears ascribable to the theoretical treatment of the latter, which involves an estimate of the electrostatic free energy as a function of degree of ionization.

Comparison of expressions for the electrostatic free energy of the DS and UCC models reveals a significant difference. The DS models use the electrostatic mutual energy of interaction *between pairs* of sites, while the UCC models use the *total* free energy of charging of cylinder. The use of infinitesimal charge elements in the latter means that a part of this charging energy involves a self-energy of creating the finite charged sites of the polyion, which is omitted in the pairwise calculation, or, more precisely, is included in the free energy of ionization of the COOH groups. This contribution leads to an overestimate of the free energy change appropriate to the removal of the proton following ionization and hence to too large a value of $m$ in the UCC case.

**Conclusions.** The electrophoretic transport of wormlike cylinders has been treated by the Burgers method in terms of the hydrodynamic chain model of Yamakawa and Fujii. The treatment, which neglects ion-atmosphere relaxation effects, predicts somewhat higher mobilities at low ionic strength for the wormlike chain than for the rigid cylinder of the same radius. This effect results from the shorter average distances between charge sites in the former. Numerical calculations of mobilities for hyaluronate are based on parameters derived from hydrodynamic measurements with use of the same chain model and otherwise involve no adjustable parameters. When corrections, based on the UCC model, for the nonlinear PB potential and ion-atmosphere relaxation are included, experimental data for hyaluronate and for polysaccharides containing one charge per hexose subunit are fitted satisfactorily.

## Addendum

I wish to express my gratitude to Dr. D. Stigter, whose suggestion has led to an alternative derivation of eq 26, which is conceptually helpful in clarifying the origin of the nearly canceling terms in eq 19. The resemblance of the Oseen treatment of the spherically symmetric ion atmosphere of eqs 10–13 to that presented long ago by Onsager[46] can be made evident as follows.

In the case of a single spherical ion a point force $Q_0X\mathbf{i}$ acting on the charge $Q_0$ of eq 13 yields a (preaveraged) Oseen contribution $\mathbf{v}_3'$ to the velocity $\mathbf{v}'$ at $r = s$ given by

$$\mathbf{v}_3' = \frac{Q_0X}{6\pi\eta s}\mathbf{i} \tag{41}$$

The resultant value of $\mathbf{v}'$, when eq 41 is added to eq 13, becomes

$$\mathbf{v}' = \mathbf{v}_1' + \mathbf{v}_2' + \mathbf{v}_3' = \frac{DX\psi_s}{6\pi\eta}\mathbf{i} \tag{42}$$

This result can also be derived for the *average* liquid velocity from the exact treatment of Stokes and Onsager (D. Stigter, private communication). Equation 18 with $\mathbf{v}'' = \mathbf{v}_0 = 0$ then leads directly at $s = a$ to eq 1, from which, for the DH potential at $r = a$

$$U = \frac{D\psi_aX}{6\pi\eta} = \frac{eX}{6\pi\eta(1+\kappa a)a} = \frac{eX}{6\pi\eta}\left(\frac{1}{a} - \frac{\kappa}{1+\kappa a}\right) \tag{43}$$

Equation 11 of Onsager for $V$ (=$U$) (with his eq 7 for $V_2$) would be identical with the last equality of eq 43, if the shear radius $a$ in the term $1/a$ were taken to be an "effective" Stokes radius. Onsager correctly avoided identifying the latter with an "ionic radius" estimated by some other method, because of the failure of macroscopic hydrodynamics at the dimensions of small ions, as

mentioned above in connection with Stokes' law.

The interest of this result for the present work lies in a proposed extension to a polyion model constructed, for example, of spherical beads each containing a charge site and surrounded by a spherically symmetric ion atmosphere. As a first "free-draining" approximation, each charge site $k$ can be assumed to contribute independently to the liquid velocity. The model resembles closely that discussed previously by Manning,[20] but here the proposal is to make quantitative use of eq 42 for the liquid velocity. In the KR approximation valid for long chains, the contributions $\mathbf{v}_k'$ at a chosen bead can be summed in the same spirit as for eq 19 to give

$$\frac{u'}{\xi} = \frac{DL}{Q}\sum_{k=1}^{Z}\langle\psi\rangle_k \tag{26a}$$

where the $\langle\psi\rangle_k$ are to be evaluated over the surface of the bead. As before, this procedure is supposed valid also for the *self*-potential of a bead of radius greater than 0.5 nm. Equation 26a is identical with eq 26, except for details of numerical evaluation, which should have negligible effect on the result, but are less convenient to carry out for spherical beads. An advantage is that the treatment leading to eq 26a should be valid for *any* location of the charge site in the polyion cross section, provided only that its ion atmosphere can reasonably be taken to be spherically symmetric. The conceptual advantage of using eq 42 for $\mathbf{v}_k'$ and consequent neglect of $\mathbf{v}_k''$ is that the hydrodynamic interaction terms do not appear as such, and the near cancellation of the first two terms in eq 19 is seen to result from the combined effect on $\mathbf{v}'$ of *each* charge site and *its own* ion atmosphere.

The latter point is of interest in connection with the question whether the neglect of fluctuations in hydrodynamic interactions implied by preaveraging the Oseen tensor in eq 16 for $\mathbf{v}''$ will lead to errors in theoretical estimates of $u'$ similar to those (up to 15%) attributed to such neglect in the case of the translational diffusion coefficient by experimental[47] and theoretical[43,48,49] results. Since a similar preaveraging occurs for $\mathbf{v}'$ from the ion atmosphere term in eq 10 and since near cancellation occurs for the first two terms in eq 19, the question becomes to what extent preaveraging affects this situation and, in particular, the residual term in the electrostatic potential in eq 26 or 26a. Further calculations, perhaps involving dynamic simulations, would seem to be needed to clarify this point.

## Appendix A

The integration procedure of Schlitt,[28] originally developed to provide numerical solutions to the KR integral equation,[21] can be applied to provide a more exact solution of eq 19 than that provided by eq 26, which employed the KR approximation. The integral eq 19 may be rewritten at any $p$ as

$$\int_0^L K(|p-q|)[\langle f(q)\rangle - \langle f(p)\rangle]\,dq + \langle f(p)\rangle g(p) - XQ_k\sum_{k=1}^{Z}\langle|\mathbf{R}-\mathbf{r}|^{-1}\rangle_k + DX\sum_{k=1}^{Z}\langle\psi\rangle_k = 6\pi\eta U \tag{A1}$$

where $g(p)$ is defined in analogous fashion to $g(q_k)$ in eq 23. Division by $g(p)$, which does not vanish for any $p$, and by $6\pi\eta U$ leads to

$$\frac{\int_0^L K(|p-q|)[\phi(q)-\phi(p)]\,dq}{g(p)} + \phi(p) = \frac{1}{g(p)} + \frac{\xi}{u'}\frac{L}{Zg(p)}\left(\sum_{k=1}^{Z}\langle|\mathbf{R}-\mathbf{r}|^{-1}\rangle_k - \frac{D}{e}\sum_{k=1}^{Z}\langle\psi\rangle_k\right) \tag{A2}$$

$$\phi(p) \equiv \langle f(p)\rangle/6\pi\eta U \tag{A3}$$

The function $g(p)$ may be evaluated analytically when $K(z)$ is given as an integrable function. After change of integration variable from $q$ to $t \equiv 2q/L - 1$, with corresponding integral limits, $t = -1$ to $t = 1$, the integral in eq 28 can be conveniently performed by Gaussian quadrature with tabulated[32] values of $t$ and the weighting factor $w$, so that

$$\frac{\frac{L}{2}\sum_{j=1}^{M}K_{ij}(\phi_j-\phi_i)w_j}{g(p)} = -\phi_i + \lambda_i - A_{i0}\phi_0 \qquad (j \neq i) \tag{A4}$$

$$A_{i0} \equiv -\frac{1}{g(p)}\frac{L}{Z}\left(\sum_{k=1}^{Z}K_{ik} - \frac{D}{e}\sum_{k=1}^{Z}\langle\psi\rangle_{ik}\right) \tag{A5}$$

$$\lambda_i \equiv g(p)^{-1} \qquad \phi_0 \equiv \xi/u' \tag{A6}$$

In eqs A4–A6 the pairs of points $i,j$ are chosen as the Gaussian quadrature abscissae of coordinates $p,q$, respectively, for the $M$-point integration. The coefficients $K_{ij}$ in eq A4 represent values of $K(|p-q|)$ and the variables $\phi_i$ and $\phi_j$ values of $\phi(p)$ and $\phi(q)$, respectively. The $K_{ik}$ values in eq A5 differ from $K_{ij}$ only in that the points $k$ are the evenly spaced charge sites, subscript $ik$ denoting a value at the plane containing point $i$ due to charge site $k$. The sum in eq A4 may be rewritten as separate sums containing $\phi_i$ and $\phi_j$ terms

$$\sum_{j=1}^{M}A_{ij}\phi_j - \phi_i\sum_{j=1}^{M}A_{ij} = -\phi_i + \lambda_i - A_{i0}\phi_0 \qquad (j \neq i) \tag{A7}$$

$$A_{ij} \equiv \frac{LK_{ij}w_j}{2g(p)} \tag{A8}$$

If the coefficient $A_{ii}$ is defined by

$$A_{ii} \equiv 1 - \sum_{i\neq j}A_{ij} \tag{A9}$$

eq A7 reduces to the set of linear equations

$$\sum_{j=0}^{M}A_{ij}\phi_j = \lambda_i \qquad (i = 1, 2, ..., M) \tag{A10}$$

where the sum now includes $j = i$.

The remaining equation needed to solve for the $M+1$ variables $\phi_j$ is the force balance, eq 15. When $\mathbf{f}(p)$ is written $\langle f(p)\rangle\mathbf{i}$ and $\mathbf{E}_0 = X\mathbf{i}$, eq 15 becomes

$$6\pi\eta U\int_0^L\phi(p)\,dp = ZQ_kX = ZeX \tag{A11}$$

Evaluation of the integral by $M$-point Gaussian quadrature, as for eq A4, then leads to

$$\frac{L}{2}\sum_{j=1}^{M}\phi_jw_j = \phi_0L \tag{A12}$$

where eq A6 has been used. If the coefficients $A_{0j}$ are

defined by

$$A_{0j} = w_j \quad (j = 1, ..., M) \qquad A_{00} = -2 \tag{A13}$$

eq A12 may be written in the form of eq A10

$$\sum_{j=0}^{M} A_{0j}\phi_j = \lambda_0 = 0 \tag{A14}$$

Equations A10 and A14 represent a set of $M + 1$ linear equations, which can be solved numerically for the $M + 1$ unknowns $\phi_j$ in the usual manner. By defining the $M + 1$ square matrix **A** of the coefficients $A_{ij}$ $(i, j = 0, ..., M)$ and two $(M + 1) \times 1$ column matrices, (1) the matrix $\phi$ of the unknowns $\phi_j$ and (2) the matrix $\lambda$ of the known quantities $\lambda_j$ $(j = 0, ..., M)$, eqs A10 and A14 may be written

$$\mathbf{A}\phi = \lambda \tag{A15}$$

which may be solved for $\phi$ by inverting the matrix **A**.

$$\phi = \mathbf{A}^{-1}\lambda \tag{A16}$$

## Appendix B

The potential $\psi_k$ due to a point charge $q_k$ located on the surface $r = a = b$ of a dielectric cylinder as defined in the text is given, according to the solution of Skolnick and Fixman,[34] in cylindrical coordinates $(z, r, \alpha)$ by

$$\psi_k = \frac{q_k}{4\pi^2}\sum_{m=-\infty}^{\infty}\int_{-\infty}^{\infty} dk\, g_m \exp(im\alpha + ikz) \tag{B1}$$

where $g_m(k)$ depends on $\kappa$ and $k$. The average surface potential $\langle\psi\rangle_k$ specified in eq 19 may readily be obtained by averaging $\psi_k$ at $r = a$ and any $z$ over the angular coordinates $\alpha$. The integral $\langle\psi\rangle_k = \int\psi_k\, d\alpha$ from $\alpha = 0$ to $\alpha = 2\pi$ vanishes for all $m$ except $m = 0$. The integral $\phi(q_k)$ defined in eq 24 then becomes, for a cylinder of infinite length

$$\phi(q_k) = \int_{-\infty}^{\infty}\langle\psi_k\rangle\, dp = \frac{q_k}{4\pi^2}\int_{-\infty}^{\infty} dk \int_{-\infty}^{\infty} g_0(k)\exp(ikz)\, dz \tag{B2}$$

Since $g_0(k)$ is independent of $z$, the $\delta$ function

$$\delta(k) = \frac{1}{2\pi}\int_{-\infty}^{\infty}\exp(ikz)\, dz \tag{B3}$$

may be substituted to give

$$\phi(q_k) = \frac{q_k}{2\pi}\int_{-\infty}^{\infty} dk\, g_0(k)\delta(k) \tag{B4}$$

The integral properties of the $\delta$ function permit expression of eq B4 as

$$\phi(q_k) = \frac{q_k g_0(0)}{2\pi} \tag{B5}$$

Evaluation of $g_0(0)$ at $k = 0$ (eqs II.8–II.10, ref 35) gives

$$g_0(0) = \frac{4\pi K_0(x_0)}{Dx_0 K_1(x_0)} \tag{B6}$$

where $x_0 \equiv \kappa a$ and $K_0(x_0)$ and $K_1(x_0)$ are modified Bessel functions of the second kind. Substitution of eqs B5 and B6 into eq 26 leads to

$$u' = 2\xi\frac{K_0(x_0)}{x_0 K_1(x_0)} \tag{B7}$$

## References and Notes


(1) Cleland, R. L. *Macromolecules* **1991**, preceding paper in this issue.
(2) Cleland, R. L.; Wang, J. L.; Detweiler, D. M. *Macromolecules* **1982**, *15*, 386.
(3) Yamakawa, H.; Fujii, M. *Macromolecules* **1973**, *6*, 407.
(4) Cleland, R. L. *Macromolecules* **1984**, *17*, 634.
(5) Debye, P.; Hückel, E. *Phys. Z.* **1923**, *24*, 305.
(6) Hückel, E. *Phys. Z.* **1924**, *25*, 204.
(7) Henry, D. C. *Proc. R. Soc. London* **1931**, *A133*, 106.
(8) Onsager, L. *Phys. Z.* **1927**, *28*, 277.
(9) Overbeek, J. T. G.; Wiersema, P. H. In *Electrophoresis*; Bier, M., Ed.; Academic: New York, 1967; Vol. 2, Chapter 1.
(10) Wiersema, P. H.; Loeb, A. L.; Overbeek, J. T. G. *J. Colloid Interface Sci.* **1966**, *22*, 78.
(11) Manning, G. S. *J. Chem. Phys.* **1969**, *51*, 924.
(12) von Smoluchowski, M. *Bull. Acad. Sci. Cracovie* **1903**, 182.
(13) Gorin, M. L. In *Electrophoresis of Proteins*; Abramson, H. A., Moyer, L. S.; Gorin, M. L., Eds.; Reinhold: New York, 1942; Chapter 5.
(14) Schellman, J. A.; Stigter, D. *Biopolymers* **1977**, *16*, 1415.
(15) de Keizer, A.; van der Drift, W. P. J. T.; Overbeek, J. T. G. *Biophys. Chem.* **1975**, *3*, 107.
(16) Stigter, D. *J. Phys. Chem.* **1978**, *82*, 1417.
(17) Hermans, J. J.; Fujita, H. *Proc. K. Ned. Akad. Wet.* **1955**, *B58*, 182.
(18) Hermans, J. J. *J. Polym. Sci.* **1955**, *18*, 527.
(19) Overbeek, J. T. G.; Stigter, D. *Recl. Trav. Chim. Pays-Bas* **1956**, *75*, 543.
(20) Manning, G. S. *J. Phys. Chem.* **1981**, *85*, 1506.
(21) Kirkwood, J. G.; Riseman, J. *J. Chem. Phys.* **1948**, *16*, 565.
(22) Kirkwood, J. G. *J. Polym. Sci.* **1954**, *12*, 1.
(23) Cleland, R. L. *Biopolymers* **1984**, *23*, 647.
(24) Kratky, O.; Porod, G. *Recl. Trav. Chim. Pays-Bas* **1949**, *68*, 1106.
(25) Yamakawa, H. *Modern Theory of Polymer Solutions*; Harper and Row: New York, 1971; p 349.
(26) Rutgers, A. J.; Overbeek, J. T. G. *Z. Phys. Chem.* **1936**, *A177*, 29.
(27) Burgers, J. M. *Second Report on Viscosity and Plasticity of the Amsterdam Academy of Sciences*; Nordemann: New York, 1938.
(28) Schlitt, D. W. *J. Math. Phys.* **1967**, *9*, 436.
(29) Yamakawa, H.; Fujii, M. *Macromolecules* **1974**, *7*, 128.
(30) Cleland, R. L. *Biopolymers* **1971**, *10*, 1925.
(31) Cleland, R. L. *Macromolecules* **1982**, *15*, 382.
(32) Abramowitz, M.; Stegun, I. A. *Handbook of Mathematical Functions*; Dover: New York, 1972; p 916.
(33) Manning, G. S. *Acc. Chem. Res.* **1979**, *12*, 443.
(34) Hill, T. L. *Arch. Biochem. Biophys.* **1955**, *57*, 229.
(35) Skolnick, J.; Fixman, M. *Macromolecules* **1978**, *11*, 867.
(36) Bailey, J. M. *Biopolymers* **1973**, *12*, 559.
(37) Robinson, R. A.; Stokes, R. H. *Electrolyte Solutions*, 2nd ed.; Butterworths: London, 1970; (a) p 237; note that their $a = 2r_i$; (b) Appendix 6.2, p 465; (c) pp 123–126.
(38) Stigter, D. *J. Colloid Interface Sci.* **1975**, *53*, 296.
(39) Stigter, D. *J. Phys. Chem.* **1979**, *83*, 1663.
(40) Klein, S. D.; Bates, R. G. *J. Solution Chem.* **1980**, *9*, 289.
(41) Flory, P. J. *Principles of Polymer Chemistry*; Cornell University: Ithaca, NY, 1953; p 310.
(42) Yamakawa, H.; Yoshizaki, T. *Macromolecules* **1980**, *13*, 633.
(43) Fixman, M. *J. Chem. Phys.* **1983**, *78*, 1594.
(44) Tuffile, F. M.; Ander, P. *Macromolecules* **1975**, *8*, 789.
(45) Katchalsky, A.; Shavit, N.; Eisenberg, H. *J. Polym. Sci.* **1954**, *13*, 69.
(46) Onsager, L. *Phys. Z.* **1926**, *27*, 388.
(47) Schmidt, M.; Burchard, W. *Macromolecules* **1981**, *14*, 210.
(48) Zimm, B. H. *Macromolecules* **1980**, *13*, 592.
(49) Fixman, M. *J. Chem. Phys.* **1986**, *84*, 4080.